Curr Cardiovasc Imaging Rep (2014) 7:9286
DOI 10.1007/s12410-014-9286-9

INTRAVASCULAR IMAGING (E REGAR AND U LANDMESSER, SECTION EDITORS)

Intracoronary Optical Coherence Tomography: Insights from Clinical Research—What Do We Need to Learn?

Maria D. Radu · Henning Kelbæk · Erik Jørgensen · Steffen Helqvist · Bettina Løjmand · Thomas Engstrøm · Kari I. Saunamäki

Published online: 22 July 2014

Abstract Optical coherence tomography (OCT) is a high-resolution technology for imaging of biological tissues that has shown tremendous potential for intracoronary use. Based on near-infrared light rather than ultrasound, catheter-based OCT provides cross-sectional images of the vessel wall and related devices in a histology-like manner. At present, OCT is primarily being used in research to better characterize and understand the pathophysiology of vulnerable plaques and to study the acute and long-term effects of coronary stent implantation. The present review provides the interventional cardiologist with a summary of the clinical research involving OCT, with an emphasis on specific challenges and how these may be overcome to promote a shift from the mainly research application of this technology, to a wider adoption in clinical practice.

Keywords Optical coherence tomography · Clinical research · Plaque characterization · Thin-cap fibroatheroma · OCT-guided stent implantation · Stent strut apposition · Stent strut coverage · Stent edge dissection · Artefacts

Introduction

Since the beginning of interventional cardiology, coronary angiography has been the reference modality to assess the severity of coronary lesions and guide stent implantation. With growing knowledge about the pathophysiology of atherothrombosis and stent failure, it has become of interest to visualize in vivo various processes taking place at the level of the coronary vessel wall for improving cardiovascular outcomes [1, 2]. Intracoronary imaging technologies overcome the lumenographic limitations of angiography by enabling a pathology-like cross-sectional view of the vessel wall and implanted devices. Although intravascular ultrasound (IVUS) has provided valuable insights into the dynamic nature of atherosclerosis [3, 4] and the causes of stent failure and how these may be prevented [5, 6], the technology is limited by an insufficient axial resolution (100–250 μm) and poor ability to differentiate between various tissue components, preventing the visualization of important plaque- and stent features. The introduction of intracoronary optical coherence tomography (OCT) has opened the door to a new world in interventional cardiology. With a near-histologic resolution of 10–20 μm, this near-infrared light-based technology offers a significantly improved visualization of plaque characteristics (eg, fibroatheromas, fibrocalcific, and fibrous plaques) and stent-related features [7, 8]. It is, therefore, expected that OCT will facilitate the identification of patients at risk of coronary events, and assist in the individualization of treatment strategy by guiding the selection and optimization of appropriate intervention. The present review provides an update of the latest advancements in clinical OCT research with particular focus on the thin-cap fibroatheroma (TCFA) and the importance of potential predictors of stent failure. This will be accompanied by a critical discussion of the steps that need to be taken in order to promote a shift from the mainly research application of this technology, to a wider adoption in clinical practice.

OCT for the Assessment of Atherosclerosis

Finding the Thin-Cap Fibroatheroma and Expressing its Vulnerability

Cardiovascular disease is the leading cause of morbidity and mortality world-wide [9] and represents the harmful

This article is part of the Topical Collection on *Intravascular Imaging*

M. D. Radu (✉) · H. Kelbæk · E. Jørgensen · S. Helqvist · B. Løjmand · T. Engstrøm · K. I. Saunamäki
Department of Cardiology, Section 2013, The Heart Center, Rigshospitalet, Blegdamsvej 9, 2100 Copenhagen, Denmark
e-mail: maria_d_radu@yahoo.com

consequences of atherosclerosis. According to the current paradigm, the TCFA is the precursor lesion of ruptured plaques, which are responsible for the majority of thrombosis-mediated acute coronary syndromes (ACS) [10]. The TCFA is histologically characterized by a large necrotic core (>20 % of the total plaque area), covered by a thin fibrous cap (<65 μm) infiltrated with macrophages [10, 11]. These features including fibrous cap disruption and thrombus can be identified with OCT with a superior sensitivity compared with IVUS and angioscopy [7, 12, 13]. In an initial effort to assess plaque characteristics using OCT in vivo, Jang et al evaluated the target lesions of patients presenting with ACS and stable angina pectoris (SAP), and found that the frequency of thrombus, plaque rupture, and TCFA increased with the severity of the clinical presentation, with a concurrent decrease in the fibrous cap thickness [14]. Subsequent studies have confirmed these observations (Table 1), corroborating the mechanistic importance of plaque rupture and thrombosis in ACS, and suggesting that these unfavorable features together with the proposed precursor TCFA can also be found in patients with stable coronary disease and in nontarget vessels. Altogether, these studies indicate that TCFAs are regularly found in culprit lesions of ST-elevation myocardial infarction (STEMI) (51 %–85 %); are relatively frequent in non (N)-STEMI (22 %–50 %); and fairly prevalent in patients with SAP (13 %–29 %) (Table 1) [13, 15–24]. The rates of plaque rupture and thrombosis follow a similar pattern, in line with previous postmortem results [25, 26], supporting the concept that target lesions in STEMI and NSTEMI are more vulnerable compared with those in SAP.

In general, OCT-detected TCFAs and plaque ruptures seem to occur with a particular clustering within the proximal 30 mm of the left anterior descending and circumflex arteries, whereas the distribution is more uniform throughout the first 70 mm of the right coronary artery [24, 27]. These findings confirm pathology data [28] and reassure that the majority of these lesions are within reach of catheter-based OCT and identifiable in a clinical setting. At a patient level, various inflammatory biomarkers may be useful for predicting the presence of these lesions in patients with clinical ischemia, and data suggest an inverse relationship between levels of these markers and the thickness and integrity of the fibrous cap [29]. Despite this association with inflammation, it has been rather surprising to find that culprit lesions in diabetic patients, by OCT, are no different from those in nondiabetics in terms of the frequency of ruptured plaques, TCFAs and fibrous cap-thickness [22, 23, 30]. Instead, diabetics often exhibit a greater extent of calcification [22, 31]. A possible explanation for this assumed paradox may be found in autopsy data suggesting that diffuse calcium deposits are more common in healed plaque ruptures compared with acute ruptures or TCFAs [32], likely representing a more advanced stage of atherosclerosis.

When it comes to expressing the vulnerability of TCFAs, attention has been focused on the utility of markers of plaque instability identified from pathology data [33]. Raffel et al observed with OCT the co-location of macrophages and TCFAs, and described an inverse relationship between the macrophage density and fibrous cap-thickness [34]. Further investigations have shown a positive correlation between both of these features and the size of the lipid pool in terms of circumferential lipid arc by OCT and positive remodeling by IVUS [35, 36]. On the one hand, these findings confirm necropsy data and support the significance of macrophages in plaque progression and destabilization [33]; and on the other, they highlight the potential value of combining various morphologic endpoints by OCT with or without IVUS, to express the degree of vulnerability and possibly the propensity for inducing clinical events. Recent data suggest that the identification of these markers may be useful in the setting of percutaneous coronary interventions (PCI) in ACS, where the presence of TCFA and a large amount of lipid by OCT have been associated with periprocedural myocardial infarction (MI), no reflow and microvascular obstruction [17, 37, 38]. Tanaka et al reported that among patients with angiographic no reflow following PCI in NSTEMI, 50 % exhibited a TCFA in the target lesion before intervention compared with 16 % in the group with normal flow (P=0.005). Although the study population included a surprisingly high proportion of patients with no reflow (17 %), it was interesting that the occurrence of this feature increased from 4.7 % to 35 % to 75 % when the lipid arc extended over 1, 2, and 3 quadrants, respectively [17]. These findings suggest a potential role of OCT in this context and are in line with recent studies using IVUS and near-infrared spectroscopy showing an association between the amount of lipid, and no reflow and periprocedural MI, respectively [39, 40].

The Natural History of Atherosclerosis

The regression and stabilization of atherosclerotic lesions are assumed to be the key mechanisms underlying the clinical benefit of lipid-lowering therapy with statins [41]. Despite the unequivocal effect of statins on LDL-cholesterol levels, a large number of IVUS studies assessing changes in plaque size by intensified statin regimens, have provided inconsistent results [42]. This may partly be attributed to variations across studies in statin type and dose, and differences in the duration of treatment and timing of imaging. However, the selection of imaging endpoint may also play a role since the presence of specific plaque characteristics may be as important as atheroma size for determining the risk of these lesions to cause events. Consistent with this concept, Stone et al used virtual histology (VH)-IVUS in patients treated for ACS to examine the clinical evolution of atherosclerosis while on standard medical treatment (~85 % receiving statins). They observed

that 51 % of the nonculprit lesions associated with clinical events within a median of 3.4 years exhibited a VH-IVUS-defined TCFA at baseline while the estimated Kaplan-Meyer event rate for a VH-TCFA to cause a clinical event was only 4.9 %. Instead they found a plaque burden >70 % to be the best predictor of events during the follow-up period [43]. Among the many possible explanations of the unexpected absence of a stronger signal from the former is the fact that the VH-TCFA definition relies on a composite of three separate criteria rather than a direct identification of TCFAs, that when fulfilled, are thought to represent a surrogate for a histologic TCFA [44].

Based on direct visualization of the thin fibrous cap, Takarada et al monitored with OCT lipid-rich nonculprit lesions in the target vessels of patients with STEMI and NSTEMI and observed at 9 months a significant increase in the fibrous cap thickness both in patients adhering to standard statin therapy (150 ±110 μm to 250 ±120 μm, $P<0.001$) and those not taking statins (153 ±116 μm to 179 ±124 μm, $P<0.01$ [45, 46]. In patients also assessed with IVUS, total atheroma volume remained stable at follow-up [46]. These findings may indicate that plaque stabilization in terms of increases in fibrous cap thickness may precede regression in total plaque volume–a hypothesis that seems reasonable considering that atherogenesis is a slowly developing process.

As opposed to this, Uemura et al sought to specifically assess the potential predictors of plaque progression using an unusual study design where they divided patients into those having lesions that at 6–9 months follow-up exhibited angiographic progression (28.8 % to 61.4 % diameter stenosis, $P<0.05$), and those without angiographic progression (~29 % diameter stenosis), and compared OCT findings at baseline. Although this definition of progression implies a certain selection bias and inevitably overlooks plaques progression that passes unnoticed by angiography (due to positive remodeling), they observed that "progressed" lesions (mainly angiographically silent) had a higher incidence of various vulnerable features at baseline, including TCFAs (77 % vs 14 %, $P<0.01$, respectively) [47]. In spite of the limitations of this study, these data are the first to associate lesion progression in vivo with TCFA. Nevertheless, they also raise the important question whether silent morphometric lesion progression with/without cap rupture and thrombosis would benefit from preventive intervention. Although the pursuit to establish the prognostic value of using OCT to identify vulnerable features has only begun, concern about the assumed threat of TCFAs has already spurred innovative attempts of plaque sealing using self-expanding nitinol stents and bioresorbable polymer scaffolds [48, 49•]. The long-term safety and efficacy of these approaches, not least in comparison with high-dose statin therapy, need however, to be evaluated before they can be considered in the clinical routine.

Challenges in Diagnosing TCFAs and Emerging Solutions

Although the above data are exciting, recent reports have drawn attention to a number of factors that may complicate a correct diagnosis of thin- and thick-cap fibroatheromas [50, 51]. One of these relates to the capability of OCT to differentiate between lipid and nonlipid tissue, which although generally good, has been associated with misinterpretation between plaque types [7, 52–54]. Accordingly, the signal-poor center of fibrocalcific plaques is often mistaken for a lipid pool because of insufficient attention to the appearance of the border between the bright fibrous tissues adjoining the signal-poor regions. Of note, this border is sharp in fibrocalcific plaques and diffuse in fibroatheromas (Fig. 1) [55]. Furthermore, deeply located fibrous and fibrocalcific plaques may be mistaken for lipid pools because of a limited tissue penetration of OCT [53] in combination with the natural light attenuation that follows with increasing distance from the OCT catheter.

Another important differential diagnosis of TCFAs is the presence of macrophages (Fig. 1), which by OCT are identified as punctate, highly backscattering (ie, bright) structures with significant signal attenuation [12]. Because of the similarities in optical properties, thin layers of macrophages close to the luminal surface can mimic the appearance of TCFAs [56•]. Even though the incidence of macrophage accumulations in different lesion types and clinical settings, and to what extent they interfere with the evaluation of TCFAs remains unknown, it is desirable to identify means that can aid in distinguishing the two, not least as macrophages are increasingly assessed in parallel with TCFAs [34, 47]. Factors that may further impede a correct diagnosis of TCFAs include vessel-related features and various artefacts (Fig. 1) [56•, 57•].

In addition to these qualitative aspects, concern has been raised about the quantitative part of the TCFA assessment [51]. In studies performed thus far, this has involved the somewhat subjective manual delineation of the thin fibrous cap—a crucial step in the distinction between thin- and thick-cap fibroatheromas. This particular issue together with issues pertaining to the selection of cut-off value to define a thin cap have previously been discussed in more detail [51]. Taken together, the above points highlight the need for a cautious assessment of possible TCFAs and suggest that studies performed until now be interpreted in light of these potential sources of error. Endeavors have already been initiated to address various challenges including an international consensus for standardization of OCT terminology and image assessment, along with documents focusing on the pitfalls in OCT image interpretation [56•, 58••]. As for the particular identification of lipid pools and necrotic cores, recent

Table 1 Optical coherence tomography findings in target and nontarget vessels in various clinical settings

Author	Population	STEMI			NSTEMI			SAP		
		Rupture	Thrombus	TCFA	Rupture	Thrombus	TCFA	Rupture	Thrombus	TCFA
Jang et al, [14]	*n*=20, STEMI *n*=20, NSTEMI *n*=17, SAP	25 %	20 %	72 % (47 μm)	15 %	25 %	50 % (54 μm)	12 %	35 %	20 % (103 μm)
Kubo et al, [13]	*n*=30, STEMI	73 %	100 %	83 % (49±21 μm)						
Fuji et al, [15]	*n*=35, STEMI *n*=20, SAP (3-vessel OCT)	46 % vs 31 %*	95 % vs 45 %*	77 % vs 77 %*				10 % vs 15 %*	25 % vs 15 %*	25 % vs 30 %*
Sawada et al, [16]	*n*=56, SAP (82 vessels)									29 %
Tanaka et al, [17]	*n*=83, NSTEMI				52 %	82 %	22 %			
Kubo et al, [18]	*n*=26, STEMI *n*=16, SAP	77 % vs 12 %**	100 % vs 8 %**	85 % (57±12 μm) vs 38 % (111±65 μm)**				7 % vs 6 %**	0 % vs 0 %**	13 % (180±65 μm) vs 6 % (181±70 μm)**
Toutouzas et al, [19]	*n*=55, STEMI	49 %	65 %	51 %						
Ino et al, [20]	*n*=40, STEMI *n*=49, NSTEMI	70 %	78 %	78 % (55±20 μm)	47 %	49 %	27 % (109±55 μm)			
Niccoli et al, [22]	*n*=72, NSTEMI				44 %	42 %	43 % (~61 μm)			
		Rupture***	Thrombus***	TCFA***						
Fukunaga et al, [23]	*n*=29, STEMI *n*=41, NSTEMI (30 % diabetics)	47 % vs 31 %**		79 % (~57±6 μm) vs 77 %**						
Toutouzas et al, [24]	*n*=42, STEMI *n*=15, NSTEMI *n*=10, UAP	67 %	70 %	67 % (42±14 μm)						

NSTEMI non-STEMI, *SAP* stable angina pectoris, *STEMI* ST elevation myocardial infarction, *TCFA* thin-cap fibroatheroma, *UAP* unstable angina pectoris

Data are for target vessels unless otherwise specified. (*) data are for nonsignificant non-target vessels; (**) data are for significant nontarget lesion; (***) data are for a combination of acute clinical settings

studies have proposed that the combination of OCT with other intracoronary modalities such as VH-IVUS may increase the accuracy of plaque characterization [54, 59]. Additional improvements are expected from quantitative analysis methods involving measurement of signal intensity and attenuation, which may not only assist in tissue characterization but also provide substrate for automatic segmentation of the fibrous cap [55, 60, 61]. Altogether, these advancements are expected to facilitate the development of methods that take advantage of the large amount of information provided by OCT, and eventually clarify the diagnostic benefits of OCT in the clinical imaging of atherosclerosis.

OCT for the Assessment and Prevention of Stent Failure

OCT to Identify Causes of Stent Failure—Focus on Stent Thrombosis

Stent implantation is the preferred treatment of coronary artery stenosis and performed annually in more than 1 million patients world-wide [62]. The long-term success depends on a combination of the quality of implantation and the subsequent vascular responses to the device, which if optimal leads to the incorporation of the stent into the vessel wall by means of a protective neointima [63]. Despite improvements in implantation techniques, stent design, antiplatelet therapy, and thereby clinical results, restenosis, and stent thrombosis (ST) remain two principal causes of stent failure. Because of the potentially life-threatening nature of the latter, with data indicating a progressively increased risk with time in early-generation drug-eluting stents (DES) [64, 65], the pathophysiology of ST and how this may be modified has attracted particular interest and will be the focus of the rest of this review.

The division of ST into early (<30 days), late (30 days–1 year), and very late (>1 year) events is not merely arbitrary but also reflects the underlying mechanisms, which vary with the time from implantation (Fig. 2) [66]. Early ST is mainly associated with factors related to the technical aspects of stent implantation including incomplete stent expansion, malapposition, edge dissections, and plaque protrusion [67]. As opposed to this, the mechanisms of late and very late ST primarily involve poor vascular healing with incomplete neointimal coverage, malapposition, chronic inflammation, and as recently suggested, disease progression with neoatherosclerosis and plaque thrombosis [68–71]. Despite data suggesting that IVUS-guided stent implantation, by means of specific criteria, may lower the risk of ST and other clinical events [72], the implementation in the clinical routine has been modest primarily because of a lack of solid scientific data in support of IVUS-guided PCI [73]. With OCT offering a clearer and more accurate visualization of relevant morphologic features, it is expected that this modality will provide additional insights into the prevention of ST.

Until recently, the direct study of the causes of stent thrombosis using OCT was confined to a number of case reports. Lately, Guagliumi et al systematically examined 18 patients with late ST (median time to event 615 days) in DES, and observed that compared with matched controls, these patients exhibited a significantly higher percentage of uncovered and malapposed struts [74•]. More recently, two independent groups reported that patients with very late ST (median 5–10 years) in both bare-metal stents (BMS) and DES exhibited high rates of in-stent neoatherosclerosis with plaque rupture [70, 71], which occurred later in the patients with vs without this finding [71]. These initial results are in line with previous autopsy and IVUS reports [68, 69, 75], confirming the feasibility of using OCT to study ST.

OCT to Guide PCI

The desire to learn how to prevent ST beyond what was possible with IVUS has motivated the evaluation of the capability of OCT to guide stent implantation, of which we will here focus on morphologic findings related to the procedure. Using criteria inspired by previous IVUS studies, Imola et al were the first to apply OCT in this setting and reported that OCT pre-intervention elicited stent implantation in 24 of 40 (60 %) patients with angiographically hazy or intermediate lesions (due to minimal lumen area <3.5 mm^2, thrombus or plaque ulceration); and led to additional intervention in 24 of 74 (32 %) patients after stent implantation (15 postdilatations due to malapposition >200 μm, prolapse or underexpansion; 9 additional stent implantations due to edge dissections) [76]. At a mean follow-up of 4.6 months, one patient experienced restenosis in a target vessel (baseline findings not reported). In parallel, however, without explicit intervention-criteria and clinical follow-up, Viceconte et al observed that OCT-evaluation of stent deployment in 108 patients led to additional postdilatation and stent implantation in 30 % and 15 % of cases, respectively [77]. Prati et al further compared patients where PCI was guided by angiography alone or in conjunction with OCT (335 patients in each group) following similar criteria as above, and observed comparable rates of OCT-triggered intervention (22.1 % and 12.6 % of 335 patients received additional balloon dilatation and stent implantation, respectively). At 12 months, authors observed a higher occurrence of cardiac death and the composite cardiac death/myocardial infarction in the angiography-guided group; however, as this was not followed by a similar difference in target lesion revascularization, the mechanisms of these findings remain unclear [78].

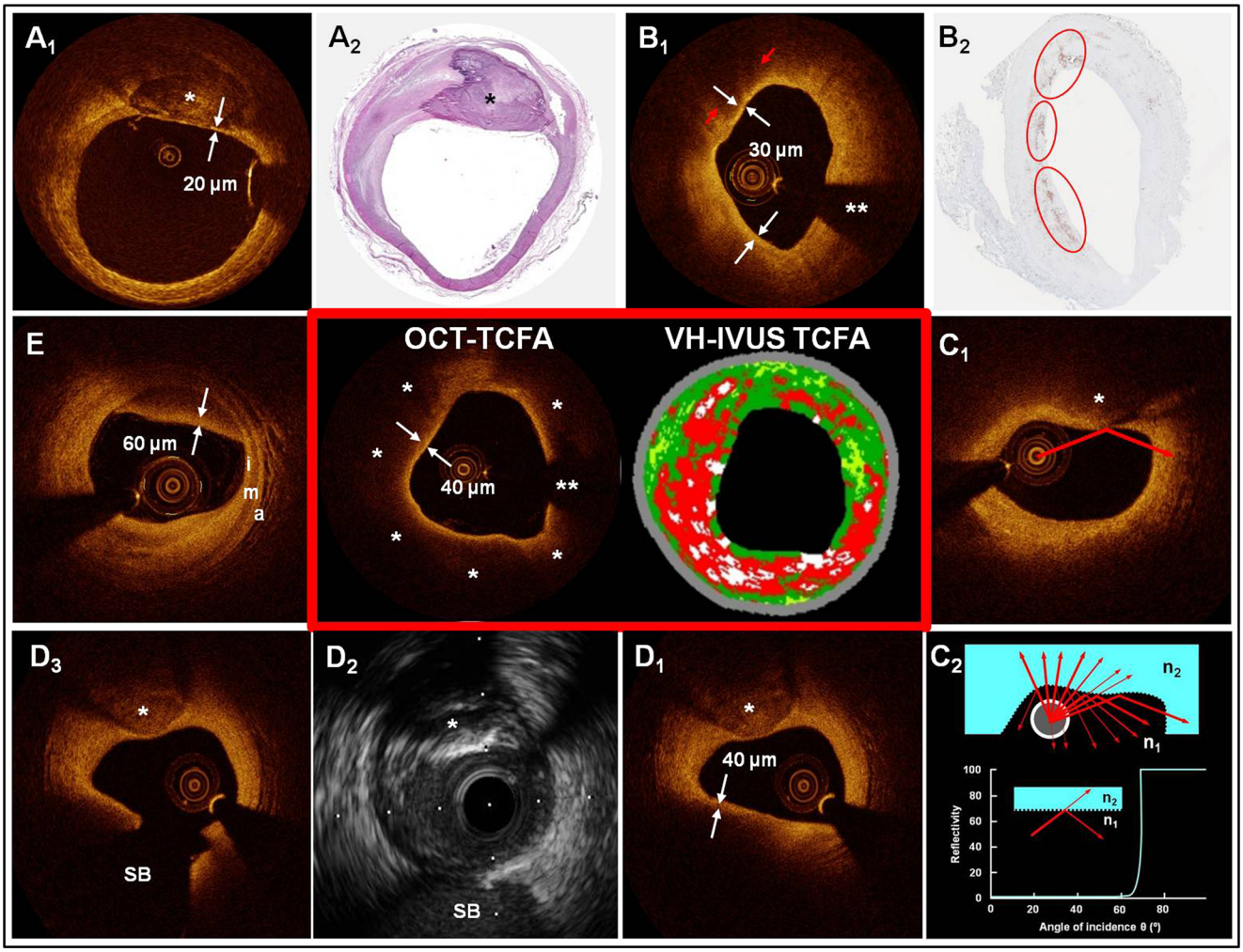

Fig. 1 Differential diagnoses for thick-cap fibroatheromas visualized with optical coherence tomography. The red box shows a representative example of a thin-cap atheroma (TCFA) as visualized with optical coherence tomography (OCT) (mid left panel), with a corresponding cross-section by virtual-histology intravascular ultrasound (VH-IVUS) (mid right panel). The TCFA by OCT is seen from 12–11 o'clock as a bright thin layer adjacent to the lumen (white arrows at 10 o'clock) overlying a signal poor region (*) representing the thin fibrous cap and lipid pool/necrotic core, respectively. Of note, the transition from the bright to signal-poor region is diffuse. The TCFA-diagnosis is supported by VH-IVUS showing necrotic core (red regions) at the corresponding sites. The discontinuation in the vessel lumen at 4 o'clock (**) is caused by a guidewire shadow, and should not be confused with a side branch. Panel $A_{1\text{-}2}$ show a fibrocalcific plaque at 12–2 o'clock by OCT (A_1) and corresponding histology (A_2, hematoxylin-eosin). Of note, the signal-poor calcified region is by OCT sharply delineated and, therefore, the thin signal-rich layer should not be considered a fibrous cap. In panel B_1 we see at 7, 9, and 11 o'clock, signal-poor regions with overlying thin signal-rich layers. The corresponding histology section (B_2, CD68 immunoperoxidase) indicates the presence of macrophages at the corresponding sites (red rings). The differentiation from a TCFA can be made by inspection of the borders of the signal-poor regions (red arrows), which in the case of macrophages are relatively sharply delineated in the direction of the infrared light radiating from the catheter. Panel C_1 shows an example of the artefacts tangential signal drop-out and interface reflectivity – both related to catheter marginalization. With the former, the OCT light almost parallels the vessel wall with less light entering the tissue causing dark regions, which may be misinterpreted as lipid pools (*). The consequence of the latter can be seen at 1 o'clock where the optical beam (red arrow) is completely reflected at the vessel interface when the incidence angle of the light approaches 70°, which is the cut-off for total light reflection (B_2) when using contrast-medium as flush. Panel D_1 shows an OCT cross-section containing of 2 dark regions at 7 and 11 o'clock. The latter corresponds to calcium (*), as discussed in panel A_1, however, the former could be diagnosed as a TCFA because of the diffuse delineation. Nevertheless, analysis of consecutive frames reveals that this region is caused by a side branch (SB in panel D_3), which is poorly visualized in panel D_1 because of the limited tissue penetration of OCT. The corresponding IVUS cross-section in D_2 confirms this. Another differential diagnosis for a TCFA is seen in panel E at 11–2 o'clock. Close evaluation of the vessel wall reveals a trilaminar vessel wall seen best at 3 o'clock with an intima (I), media (M), and adventitia (A). By following these along the circumference it becomes clear that the bulky material at 11–2 o'clock lies on top of the luminal contour. Inspection of consecutive frames (not shown) suggests that this represents residual blood because of insufficient flush. Mid panels with TCFA and panels A-C reproduced with permission from Radu et al. Clinical Atlas of OCT, EUROPA Publishing 2012, courtesy of Bruining N, (A), Johnson T, Banz Y, (B), and mid panels from the IBIS4 trial by Räber L, Windecker S, Kelbæk H and Radu M

As for the presence of intra-stent thrombotic material by OCT after stent implantation in STEMI and NSTEMI, Di Giorgio et al evaluated the effect of OCT-directed high-pressure dilation in cases where thrombus protruded into the lumen≥200 μm. Accordingly, authors achieved a significant reduction in thrombus area when compared with the angiography-guided group, with concomitant expected increases in stent and lumen areas. Of note, both groups exhibited similar degrees of thrombus protrusion (4.3 %–16.7 % thrombus area) immediately after stent deployment (n=80 patients in total), and even though there may be a risk of distal embolization with additional balloon dilatation, the procedure proved to be safe in terms of TIMI flow [79]. At 1 year, the additional dilatation did not seem to convey any clinical benefits compared with the angiography-guided group. The above studies directly illustrate that "imperfect results" visualized with OCT during PCI generate concern for further complications and may trigger additional intervention—for which there is not yet sufficient evidence. For a better understanding of how to use OCT to guide PCI, it is crucial to know the natural history of relevant OCT-detected features.

Incidence and Natural History of "Unfavorable" Features at Baseline and Follow-up

Edge Dissections

Edge dissections have long been a subject of interest considering the association of angiographic- and IVUS-detected edge dissections with early ST [67, 80–82]. Although other studies have suggested that IVUS-detected edge dissections cause clinical events only in a minority of patients, the dramatic appearance of edge dissections by OCT—even when angiographically silent—has renewed the debate about the clinical importance of these and other (mainly) angiographically silent features. This has stimulated a number of studies (Table 2) indicating a post-PCI incidence of edge dissections between 14 %–47 % by OCT [78, 83–90], compared with historical 7 %–19 % by IVUS [91, 92], and 2 %–6 % by angiography [80, 81]. The reported OCT-detected dissections extended on average 1.4–2.9 mm along the vessel segment, with flap lengths measuring on average 0.52–1.2 mm. Between 9 % and 36 % of these edge dissections were visible by angiography (not flow-limiting), and concomitant IVUS (40 MHz transducer) used in 2 studies identified ~50 % of the OCT-detected edge dissections [85, 86]. Only 4 studies directly evaluated the natural history of edge dissections by serial analysis and found that a total of 75 of 79 examined dissections were completely healed at a follow-up of 188 days (median) in one study (n=12) and 1 year in the other studies (n=65) (Fig. 3) [85, 86, 88, 90]. Out of these 79 serially studied edge dissections, there was only one early stent thrombosis within 2 hours of intervention (details on size and other coexisting risk factors not reported). In addition to these findings, Chamié et al observed in a large cohort of patients with 106 edge dissections that those with untreated edge dissections (longitudinal extension 2.0±1.6 mm; flap length 1.1±0.7 mm) had similar outcomes at 1 year clinical follow-up as those with treated edge dissections of similar dimensions [89]. Altogether, these data suggest that OCT-detected edge dissections, which are angiographically silent in a majority of cases, are common and per se associated with a favorable clinical course.

Other signs of vessel injury including tissue prolapses, thrombus and intra-stent dissections may cause as much concern for adverse events as edge dissections. Tissue prolapses refer to convex-shaped tissue protrusions between stents struts without discontinuation of the vessel surface, whereas thrombi are identified as irregular masses with dorsal shadowing protruding into the lumen, and intra-stent dissections seen as disruptions in the luminal vessel surface in the stented segment (Fig. 3) [83]. Emerging data (Table 3) suggest that prolapses with lengths averaging 250–600 μm and intra-stent dissections with flap lengths around 450 μm are present in almost all lesions after PCI, and seem to be resolved in the majority of cases at 6–9 months [83, 85, 88, 93]. Thrombi are also common (~40 % of cases) and likewise appear to be resolved in >90 % of cases at 8 months without any adverse events [88]. With the scarce data available, final conclusions about these features cannot yet be drawn.

Malapposition

Malapposition describes the lack of contact between the stent struts and the underlying vessel wall and should not be confused with stent underexpansion denoting the minimum stent area by itself or compared with a reference. The timing of imaging relative to the index procedure allows the distinction between acute malapposition, present immediately after stent implantation; and late malapposition, detected at any other time point, which may be persistent since stent implantation, or acquired with time—a differentiation requiring serial imaging. Both types of IVUS-detected malapposition have been associated with ST [67, 69, 94], and it remains unclear which mechanisms are involved in bringing malapposed struts at risk of early and late ST. The incidence of acute OCT-detected malapposition (Table 3) amounts to 4 %–9 % struts after PCI or, using a binary definition, 25 %–75 % of lesions have been reported to exhibit ≥1 malapposed strut after stent implantation [95, 96•, 97, 98]. Acute malapposed struts seem to be more frequent in

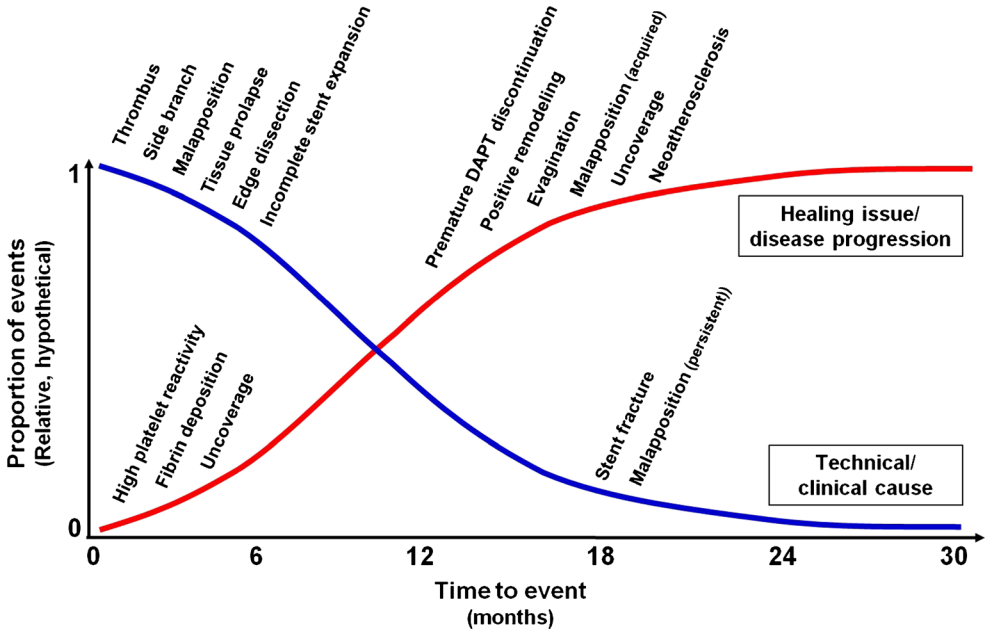

Fig. 2 Causes of stent thrombosis in relation to the index procedure. *DAPT* double antiplatelet therapy

stents implanted during ACS, at sites of stent overlap, in proximal segments and with thick struts, and correlate with the circumferential extent of vessel calcification [95, 97–100]. Serial studies indicate that the frequency of malapposition decreases significantly from baseline to moderate-term follow-up by means of growth of neointima filling the space between the strut and vessel wall (7.2 % to 4.6 % [96•] and 3.5 % to 0.5 % [101]). Compared with completely apposed struts, acute malapposed struts have been associated with delayed coverage and subclinical thrombus formation, thus, constituting a potential substrate for clinical thrombosis [96•, 101, 102•]. Among the factors determining whether malapposition will heal or not is the degree of incomplete apposition: Gutierrez-Chico et al recently observed that the likelihood of persistent malapposition increased with the distance from the vessel wall such that 95 % and 75 % of incompletely apposed struts with malapposition distances up to 350 and 850 μm were completely resolved at 6–13 months follow-up, and grossly covered in 100 % and 88 % of struts, respectively. Conversely, malapposition with distances beyond 350 and 850 μm persisted in 57 % and 100 % cases, with grossly delayed healing in 27 % and 100 % of these struts, respectively [103]. Although these numbers may appear high, it should be noted that on the one hand, residual malapposition may still resolve with additional follow-up; and on the other, that malapposition distances most often average ~250 μm [95], and these relatively small amounts of acute incomplete apposition have hitherto not been associated with any clinical events up to 1 year [96•, 97, 103].

Late acquired stent malapposition is mainly associated with positive vessel remodeling, although mechanisms such as thrombus resolution and plaque embolization have also been proposed [104]. IVUS has reported an incidence of late acquired malapposition in up to 6 % and 25 % of segments after BMS and DES implantation, respectively, with highest rates reported in first-generation sirolimus-followed by paclitaxel-eluting stents [94]. Comparable reliable OCT data are limited—something that may be ascribed the complexity of acquiring and analyzing serial OCT data together with the fact that focus with OCT mainly has been on strut coverage. Nevertheless, OCT evaluations at follow-up within randomized trials have reported that 10 % and 38 %–49 % of lesions implanted with BMS and DES, respectively, exhibit ≥1 malapposed strut at 6–13 months. At the strut level, however, unadjusted rates of malapposed struts are considerably lower, namely ~0.6 %–1.4 % per lesion up to 5 years, and have not been associated with adverse events up to the imaging follow-up [105–109].

As opposed to malapposition, stent strut coverage is the main parameter that has driven the adoption of OCT into the clinical arena. The landmark report from 2007 by Finn et al appointing the ratio of uncovered to total stent struts (RUTSS) the best morphometric predictor of late ST in DES initiated a wave of studies focused on the ability of OCT to identify very thin strut coverage (used as surrogate for neointimal coverage), with the purpose of clarifying which lesions are at risk of late ST and whether patients with these lesions would benefit from a prolonged double antiplatelet regimen [110–112, 113•].

Table 2 Summary of data on edge dissections studied with optical coherence tomography

Study	Population (incidence) ***	Clinical setting	Stent type	N Edge dissections	Location	Edge dissection size	FUP	Nat hist (serial)	Clinical events
Gonzalo, [83, 84]	73 pts 80 vessels (30 %)	STEMI: 14 % UAP: 30 % SAP: 56 %	DES: 83 %	OCT: 24 Angio: 8 (33 %)	Prox: 7 Dist: 17	Longitud: 1.4±0.8 mm Flap length: 0.74±0.44 mm	In-hospital	NA	None during in-hospital
Prati, [78]	335 pts 335 lesions (14 %)	STEMI: 26 % NSTEACS: 33 % SAP: 41 %	DES: 63 %	OCT: 47	NA	None specified, however, according to criteria, only flap lengths≥0.2 mm were included	1 y	NA	Not traceable to edge dissections
Kume, [85]	36 pts 39 lesions (31 %)	UAP: 17 % SAP: 83 % pts	DES: 80 %	OCT: 12 IVUS: 6/12 (50 %) Angio: 0	NA	Longitud: NA Flap length: 0.67±0.34 mm	188 d (98–461) *	100 % completely healed	None @ 1 mo None @ imaging FUP
Radu, [86]	57 pts 63 lesions (35 %)	NSTEACS: 70 % SAP: 30 %	DES: 100 %	OCT: 22 IVUS: 9/18 (50 %) Angio: 2 (9 %)	Prox: 6 Dist: 16	Longitud: 2.9 (1.6–2.4) ** mm Flap length: 1.2 (0.9–1.7) ** mm Depth: 0.6 (0.4–0.7) ** mm	1 y	90 % completely healed 10 % partially healed	None @ imaging FUP
Reith, [87]	73 pts 90 lesions (46 %)	ACS: 10 % SAP: 90 %	DES: 84 %	OCT: 42 Angio: 15 (36 %)	Prox: 14 Dist: 28	$Longitud_{OCT+A}$: 1.96±1.51 mm $Flap\ length_{OCT+A}$: 0.69±0.40 mm $Longitud_{OCT}$: 1.61±0.89 mm $Flap\ length_{OCT}$: 0.52±0.22 mm	NA	NA	NA
Kawamori, [88]	35 pts 40 lesions (20 %)	ACS: 6 % SAP: 94 %	DES: 100 %	OCT: 8 Angio: 0	NA	NA	8 mo	100 % completely healed	None related to EDs
Chamié, [89]	230 pts 249 lesions (43 %)	ACS: 69 % SAP: 31 %	DES: 92 %	OCT: 106 Angio: 17 (16 %)	Prox: 34 Dist: 72	Longitud: 2.0±1.6 mm Flap length: 1.1±0.7 mm	1 y	NA	Not traceable to edge dissections
Christensen, [90]	97 pts (34 %)	NA	DES: 100 %	OCT: 37 Angio: 0		Longitud: 1.9±1.0 mm Flap length: 1.1±0.6 mm	1 y	95 % completely healed	1 early ST in a leasion with ED–no details

A angiography, *DES* drug-eluting stent, *Dist* distal, *FUP* follow-up, *IVUS* intravascular ultrasound, *NA* none available, *Nat hist (serial)* natural history by serial imaging, *NSTEACS* non ST-elevation acute coronary syndrome, *OCT* optical coherence tomography, *Prox* proximal, *pts* patients, *SAP* stable angina pectoris, *STEMI* ST-elevation myocardial infarction, *UAP* unstable angina pectoris

*median (range); **median (IQR); ***Incidence of edge dissections

Data reported thus far have been recently reviewed by Gutierrez-Chico et al, in summary showing that strut coverage increases over time, with highest rates of bare struts among early-generation sirolimus- and paclitaxel-eluting stents (~6 % at 12 months for both, and 1 % at 48 months for sirolimus-eluting stents), and lowest in newer-generation DES, altogether in line with autopsy data [114, 115]. These differences in strut coverage have not yet proved to be of clinical importance.

Methodological Considerations and Future Directions

While the clinical impact of incidentally discovered malapposition and uncoverage in otherwise asymptomatic patients remains debatable, it seems obvious to evaluate these parameters as risk markers. As for the use of OCT to assess stent healing, it is notable that the resolution is in fact insufficient to detect endothelial cells (thickness <10 μm) explaining why strut coverage as opposed to endothelialization is a more appropriate feature to study with OCT. It is then important to bear in mind that the histologic term "uncovered" refers to struts lacking a coverage composed of neointimal components [111]. Struts covered with fibrin, which per definition is not "tissue", are thus, "uncovered" wherefore; the true rate of uncovered struts might be underestimated using OCT. This is supported by a comparison between OCT and histology where OCT demonstrated a sensitivity of 78 % and specificity of 96 % for the identification of uncovered struts [116]. Conveniently, it was recently shown that analysis of backscatter and attenuation data can be used to distinguish between strut coverage composed of fibrin vs neointima [113•, 116]. How to implement these advancements for a more accurate detection of strut coverage/uncoverage is currently being investigated.

Another important aspect concerns the reporting of data: most OCT studies report the presence of strut coverage in a binary fashion expressed at the cross-sectional, lesion- and sometimes at the population level, often without consideration of the hierarchical structure of the data. On the one hand, this makes it difficult to compare different studies; on the other, this way of summarizing OCT data differs from the histologic RUTSS, that when exceeding 30 % was associated with a 9-times increased odds for late ST [68]. The discrepancy in the selection of methods may be related to the fact that a RUTSS >30 % by OCT is extremely rare in asymptomatic patients and averages only ~22 % in patients imaged during clinical late ST [74•]—something which in the latter should be seen in view of the difficulty of OCT for distinguishing

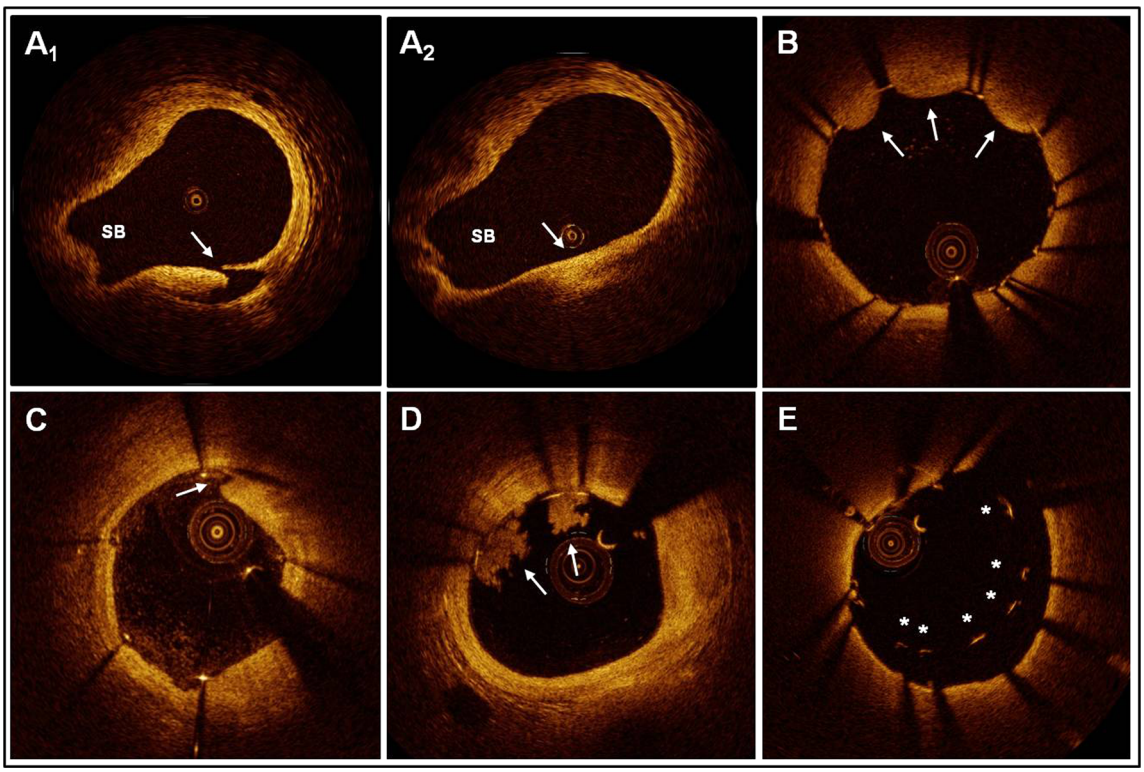

Fig. 3 Optical coherence tomography findings following stent implantation. Panel A_1 shows a stent edge dissection at 5 o'clock (arrow) in the vicinity of a side branch (SB), as visualized immediately after stent implantation. At 12-months follow-up, this was completely healed (A_2). Panels B-E show examples of tissue prolapses (B), an intra-stent dissection (C), thrombus (D), and malapposed struts (* in E)

Table 3 Summary of data on thrombus, tissue prolapses and intra-stent dissections studied with optical coherence tomography

Author	Population	Clinical setting	Stent type	Incidence	Size	FUP	Nat hist (serial)	Clinical events
Gonzalo, [83, 84]	73 pts 80 vessels	STEMI: 14 % UAP: 30 % SAP: 56 %	DES: 83 %	T: 36/80 (45 %) P: 78 sites/80 vessels ISD: 70/80 vessels	NA MPL: 254±90 μm MFL: 450±220 μm	In-hospital	NA	None
Kume, [85]	36 pts 39 lesions	UAP: 17 % pts SAP: 83 % pts	DES: 80 %	P: 25 sites/ 39 lesions	MPL: 600±210 μm	188 d (98-461)*	P: all resolved	None @ 1 mo None @ imaging UP
Kawamori, [88]	35 pts 40 lesions	ACS: 6 % SAP: 94 %	DES: 100 %	T: 15/40 (37.5 %) P: 38 sites/40 stents	NA NA	8 mo	T: Resolved in 14/15 (93 %) P: all resolved	None related to features
De Cock, [93]	50 segments	NA	DES: 100 %	P: 105 sites in 41/50 segments ISD: 268 sites in 49/50 segments	MPL**: 292±94 μm MFL**: 410±196 μm	9 mo	P: NA ISD: 92 % resolved	NA

DES drug-eluting stent, *FUP* follow-up, *ISD* intra-stent dissection, *MFL* mean flap length, *MPL* mean prolapse length, *NA* none available, *Nat hist (serial)* natural history by serial imaging, *P* prolapse, *pts* patients, *SAP* stable angina pectoris, *STEMI* ST-elevation myocardial infarction, *T* thrombus, *UAP* unstable angina pectoris

*interquartile range; **mean±SD

between thrombus and neointima during ST. Considering also that the methods for estimating the histologic RUTSS are based on a number of factors directly influenced by the ex vivo setting of histology [117], it may be discussed whether the RUTSS can reliably be extrapolated from histology to OCT, and whether it is at all the best parameter to express the future risk of late ST with OCT. Although malapposition is readily assessable with IVUS and OCT, it has attracted little attention in autopsy studies, which report a surprisingly low incidence in the setting of late ST—something that may be related to histologic processing [118]. Nevertheless, incidentally discovered malapposition by IVUS at 8 months point to an increased risk of ST and myocardial infarction at 5 years, and OCT suggests that malapposed struts even at very long-term follow-up appear to be associated with an absence of coverage [109]. Although the mechanism of malapposition in studies without serial imaging remains unknown, it may be argued that in cases of persistent acute malapposition, the mechanism of uncoverage may be related to a permanently delayed healing. However, in cases with positive remodeling this may be different: considering that lesions with uncovered malapposed struts in some instances exhibit ectatic segments with coronary evaginations, which also correlate with positive remodeling and, which suggestively represent a pre-stage to malapposition [119], it may be speculated that an absence of coverage at follow-up could also be the result of neointimal stretching and disruption during the vessel dilation occurring with progressive remodeling. Of note, Guagliumi et al observed that the only independent predictors of late ST were the length of segment with (OCT-detected) uncovered struts and (IVUS-assessed) positive remodeling—the latter supported by previous data [69, 74•]. Furthermore, Räber et al noted that of the patients examined with OCT at 5 years, four had a high density of malapposed struts and large coronary evaginations, and out of these, two patients experienced very late ST related to these regions 6 months and 1 year later [109]. We recently observed that lesions with "major" coronary evaginations beyond prespecified dimensions had a higher rate of subclinical thrombus compared with lesions without this feature (49 % vs 14 %, P=0.007)—something that may be related to local flow disturbances at the site of these ectatic regions, which in simulation studies seem to increase with increasing evagination size [119, 120]. With prospective clinical data on these features pending, it is notable that stent-related angiographic ectasias of similar dimensions at 12 months have been associated with late stent thrombosis [121].

Taken together, it may be hypothesized that a combination of established and new morphologic features by OCT with or without IVUS, fulfilling certain extent criteria with cut-offs which are yet to be determined,

may provide a better prediction of the risk of late ST rather than one predictor alone—something that seems logical when considering the pathophysiology of thrombosis from a Virchowian point of view (Fig. 4). That yet additional risk factors such as neoatherosclerosis are emerging may further complicate the estimation of thrombotic risk [70, 71]. Nonetheless, recommendations on how to analyze and report quantitative and qualitative data in relation to coronary stents together with the development of semi-automatic software to facilitate the time-consuming analysis process [122] are anticipated in a near future and will provide an indispensable basis to promote the wider adoption of OCT in clinical practice.

Conclusions

The introduction of OCT has significantly advanced our knowledge of the pathophysiology of atherosclerosis and vascular responses to stent implantation. Although we are only now beginning to understand the clinical importance of various features related to coronary stents as well as plaques, a substantial amount of work remains to establish criteria of prognostic importance both during stenting and at follow-up. The achievement of these goals depends on an increased awareness of the limitations of current methodologic concepts, which together with further developments of automated tissue characterization and stent analysis software will

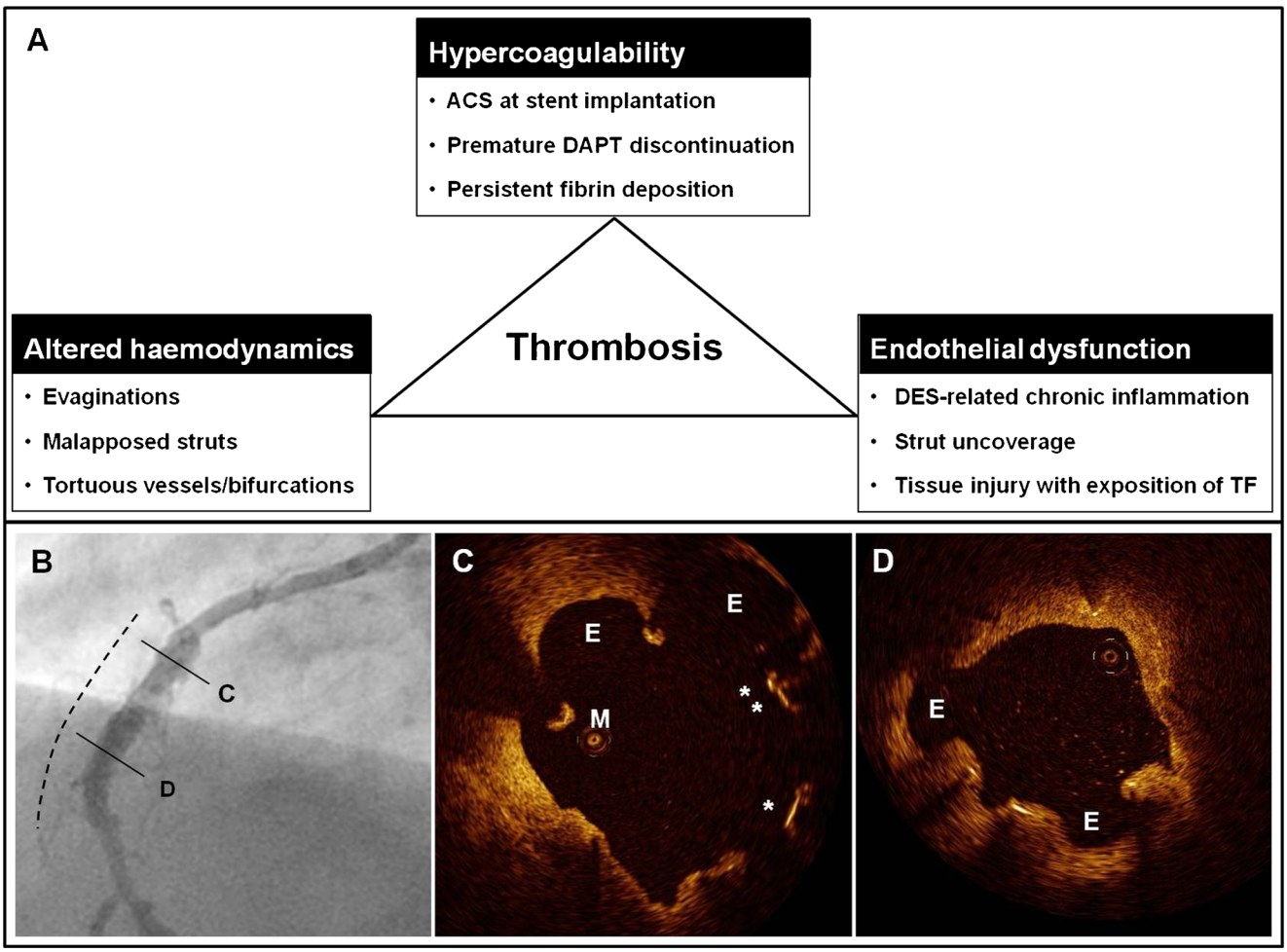

Fig. 4 Factors associated with late stent thrombosis. Panel A shows a number of factors associated with late stent thrombosis and classified according to the triad of Virchow. Panels B-C show the angiographic and OCT-findings in a case of late stent thrombosis. This 54-year-old male had a sirolimus-eluting stent implanted in the right coronary artery in the setting of a STEMI. Seventeen months later, clopidogrel was discontinued, and 27 months following stent implantation, the patient presented with an inferior STEMI. One week following thrombolysis, angiography showed peri-stent contrast staining in the previously stented segment (dashed line). OCT demonstrated evaginations (E), malapposed (M), and uncovered (*) struts, as shown in panels C-D. Please note that OCT was performed without a guide wire, which is a differential diagnosis for the malapposed strut in panel C. Reprinted from EuroIntervention 2014;10:113-23, Radu et al. Flow-disturbances in stent-related coronary evaginations: a computational fluid dynamic simulation study. Copyright 2014, with permission from Europa Digital & Publishing. *ACS* acute coronary syndrome, *DAPT* double antiplatelet therapy, *DES* drug-eluting stent, *TF* tissue factor

facilitate the accomplishment of serial studies to eventually clarify the role of OCT in interventional cardiology.

Compliance with Ethics Guidelines

Conflict of Interest Maria D. Radu, Henning Kelbæk, Erik Jørgensen, Steffen Helqvist, Bettina Løjmand, Thomas Engstrøm, and Kari I. Saunamäki declare that they have no conflicts of interest.

Human and Animal Rights and Informed Consent This article does not contain any studies with human or animal subjects performed by any of the authors

References

Papers of particular interest, published recently, have been highlighted as:
- • Of importance
- •• Of major importance

1. Muller JE, Abela GS, Nesto RW, et al. Triggers, acute risk factors and vulnerable plaques: the lexicon of a new frontier. J Am Coll Cardiol. 1994;23:809–13.
2. Schwartz RS, Huber KC, Murphy JG, et al. Restenosis and the proportional neointimal response to coronary artery injury: results in a porcine model. J Am Coll Cardiol. 1992;19:267–74.
3. Mintz GS, Painter JA, Pichard AD, et al. Atherosclerosis in angiographically "normal" coronary artery reference segments: an intravascular ultrasound study with clinical correlations. J Am Coll Cardiol. 1995;25:1479–85.
4. Jensen LO, Thayssen P, Pedersen KE, et al. Regression of coronary atherosclerosis by simvastatin: a serial intravascular ultrasound study. Circulation. 2004;110:265–70.
5. Nakamura S, Colombo A, Gaglione A, et al. Intracoronary ultrasound observations during stent implantation. Circulation. 1994;89:2026–34.
6. Colombo A, Hall P, Nakamura S, et al. Intracoronary stenting without anticoagulation accomplished with intravascular ultrasound guidance. Circulation. 1995;91:1676–88.
7. Yabushita H, Bouma BE, Houser SL, et al. Characterization of human atherosclerosis by optical coherence tomography. Circulation. 2002;106:1640–5.
8. Bouma BE, Tearney GJ, Yabushita H, et al. Evaluation of intracoronary stenting by intravascular optical coherence tomography. Heart. 2003;89:317–20.
9. Alwan A, Maclean DR, Riley LM, et al. Monitoring and surveillance of chronic non-communicable diseases: progress and capacity in high-burden countries. Lancet. 2010;376:1861–8.
10. Virmani R, Kolodgie FD, Burke AP, et al. Lessons from sudden coronary death: a comprehensive morphological classification scheme for atherosclerotic lesions. Arterioscler Thromb Vasc Biol. 2000;20:1262–75.
11. Burke AP, Farb A, Malcom GT, et al. Coronary risk factors and plaque morphology in men with coronary disease who died suddenly. N Engl J Med. 1997;336:1276–82.
12. Tearney GJ, Yabushita H, Houser SL, et al. Quantification of macrophage content in atherosclerotic plaques by optical coherence tomography. Circulation. 2003;107:113–9.
13. Kubo T, Imanishi T, Takarada S, et al. Assessment of culprit lesion morphology in acute myocardial infarction: ability of optical coherence tomography compared with intravascular ultrasound and coronary angioscopy. J Am Coll Cardiol. 2007;50:933–9.
14. Jang IK, Tearney GJ, MacNeill B, et al. In vivo characterization of coronary atherosclerotic plaque by use of optical coherence tomography. Circulation. 2005;111:1551–5.
15. Fujii K, Masutani M, Okumura T, et al. Frequency and predictor of coronary thin-cap fibroatheroma in patients with acute myocardial infarction and stable angina pectoris a 3-vessel optical coherence tomography study. J Am Coll Cardiol. 2008;52:787–8.
16. Sawada T, Shite J, Garcia-Garcia HM, et al. Feasibility of combined use of intravascular ultrasound radiofrequency data analysis and optical coherence tomography for detecting thin-cap fibroatheroma. Eur Heart J. 2008;29:1136–46.
17. Tanaka A, Imanishi T, Kitabata H, et al. Lipid-rich plaque and myocardial perfusion after successful stenting in patients with non-ST-segment elevation acute coronary syndrome: an optical coherence tomography study. Eur Heart J. 2009;30:1348–55.
18. Kubo T, Imanishi T, Kashiwagi M, et al. Multiple coronary lesion instability in patients with acute myocardial infarction as determined by optical coherence tomography. Am J Cardiol. 2010;105:318–22.
19. Toutouzas K, Tsiamis E, Karanasos A, et al. Morphological characteristics of culprit atheromatic plaque are associated with coronary flow after thrombolytic therapy: new implications of optical coherence tomography from a multicenter study. JACC Cardiovasc Interv. 2010;3:507–14.
20. Ino Y, Kubo T, Tanaka A, et al. Difference of culprit lesion morphologies between ST-segment elevation myocardial infarction and non-ST-segment elevation acute coronary syndrome: an optical coherence tomography study. JACC Cardiovasc Interv. 2011;4:76–82.
21. Nasu K, Terashima M, Habara M, et al. Impact of cholesterol metabolism on coronary plaque vulnerability of target vessels: a combined analysis of virtual histology intravascular ultrasound and optical coherence tomography. JACC Cardiovasc Interv. 2013;6:746–55.
22. Niccoli G, Giubilato S, Di Vito L, et al. Severity of coronary atherosclerosis in patients with a first acute coronary event: a diabetes paradox. Eur Heart J. 2013;34:729–41.
23. Fukunaga M, Fujii K, Nakata T, et al. Multiple complex coronary atherosclerosis in diabetic patients with acute myocardial infarction: a three-vessel optical coherence tomography study. EuroIntervention. 2012;8:955–61.
24. Toutouzas K, Karanasos A, Riga M, et al. Optical coherence tomography assessment of the spatial distribution of culprit ruptured plaques and thin-cap fibroatheromas in acute coronary syndrome. EuroIntervention. 2012;8:477–85.
25. Davies MJ, Thomas A. Thrombosis and acute coronary-artery lesions in sudden cardiac ischemic death. N Engl J Med. 1984;310:1137–40.
26. Farb A, Tang AL, Burke AP, et al. Sudden coronary death. Frequency of active coronary lesions, inactive coronary lesions, and myocardial infarction. Circulation. 1995;92:1701–9.
27. Tanaka A, Imanishi T, Kitabata H, et al. Distribution and frequency of thin-capped fibroatheromas and ruptured plaques in the entire culprit coronary artery in patients with acute coronary syndrome as determined by optical coherence tomography. Am J Cardiol. 2008;102:975–9.
28. Cheruvu PK, Finn AV, Gardner C, et al. Frequency and distribution of thin-cap fibroatheroma and ruptured plaques in human coronary arteries: a pathologic study. J Am Coll Cardiol. 2007;50:940–9.
29. Li QX, Fu QQ, Shi SW, et al. Relationship between plasma inflammatory markers and plaque fibrous cap thickness determined by intravascular optical coherence tomography. Heart. 2010;96:196–201.

30. Chia S, Raffel OC, Takano M, et al. Comparison of coronary plaque characteristics between diabetic and non-diabetic subjects: an in vivo optical coherence tomography study. Diabetes Res Clin Pract. 2008;81:155–60.
31. Feng T, Yundai C, Lian C, et al. Assessment of coronary plaque characteristics by optical coherence tomography in patients with diabetes mellitus complicated with unstable angina pectoris. Atherosclerosis. 2010;213:482–5.
32. Burke AP, Weber DK, Kolodgie FD, et al. Pathophysiology of calcium deposition in coronary arteries. Herz. 2001;26: 239–44.
33. Naghavi M, Libby P, Falk E, et al. From vulnerable plaque to vulnerable patient: a call for new definitions and risk assessment strategies: Part I. Circulation. 2003;108:1664–72.
34. Raffel OC, Tearney GJ, Gauthier DD, et al. Relationship between a systemic inflammatory marker, plaque inflammation, and plaque characteristics determined by intravascular optical coherence tomography. Arterioscler Thromb Vasc Biol. 2007;27:1820–7.
35. Raffel OC, Merchant FM, Tearney GJ, et al. In vivo association between positive coronary artery remodeling and coronary plaque characteristics assessed by intravascular optical coherence tomography. Eur Heart J. 2008;29:1721–8.
36. Rathore S, Terashima M, Matsuo H, et al. Association of coronary plaque composition and arterial remodeling: an optical coherence tomography study. Atherosclerosis. 2012;221:405–15.
37. Porto I, Di Vito L, Burzotta F, et al. Predictors of periprocedural (type IVa) myocardial infarction, as assessed by frequency-domain optical coherence tomography. Circ Cardiovasc Interv. 2012;5(89–96):S81–6.
38. Ozaki Y, Tanaka A, Tanimoto T, et al. Thin-cap fibroatheroma as high-risk plaque for microvascular obstruction in patients with acute coronary syndrome. Circ Cardiovasc Imaging. 2011;4: 620–7.
39. Lee SY, Mintz GS, Kim SY, et al. Attenuated plaque detected by intravascular ultrasound: clinical, angiographic, and morphologic features and post-percutaneous coronary intervention complications in patients with acute coronary syndromes. JACC Cardiovasc Interv. 2009;2:65–72.
40. Goldstein JA, Maini B, Dixon SR, et al. Detection of lipid-core plaques by intracoronary near-infrared spectroscopy identifies high risk of periprocedural myocardial infarction. Circ Cardiovasc Interv. 2011;4:429–37.
41. Schwartz GG, Olsson AG, Ezekowitz MD, et al. Atorvastatin for acute coronary syndromes. JAMA. 2001;286:533–5.
42. Garcia-Garcia HM, Costa MA, et al. Imaging of coronary atherosclerosis: intravascular ultrasound. Eur Heart J. 2010;31:2456–69.
43. Stone GW, Maehara A, Lansky AJ, et al. A prospective natural-history study of coronary atherosclerosis. N Engl J Med. 2011;364:226–35.
44. Garcia-Garcia HM, Mintz GS, Lerman A, et al. Tissue characterisation using intravascular radiofrequency data analysis: recommendations for acquisition, analysis, interpretation and reporting. EuroIntervention. 2009;5:177–89.
45. Takarada S, Imanishi T, Kubo T, et al. Effect of statin therapy on coronary fibrous-cap thickness in patients with acute coronary syndrome: assessment by optical coherence tomography study. Atherosclerosis. 2009;202:491–7.
46. Takarada S, Imanishi T, Ishibashi K, et al. The effect of lipid and inflammatory profiles on the morphological changes of lipid-rich plaques in patients with non-ST-segment elevated acute coronary syndrome: follow-up study by optical coherence tomography and intravascular ultrasound. JACC Cardiovasc Interv. 2010;3:766–72.
47. Uemura S, Ishigami K, Soeda T, et al. Thin-cap fibroatheroma and microchannel findings in optical coherence tomography correlate with subsequent progression of coronary athermanous plaques. Eur Heart J. 2012;33:78–85.
48. Wykrzykowska JJ, Diletti R, Gutierrez-Chico JL, et al. Plaque sealing and passivation with a mechanical self-expanding low outward force nitinol vShield device for the treatment of IVUS and OCT-derived thin cap fibroatheromas (TCFAs) in native coronary arteries: report of the pilot study vShield Evaluated at Cardiac hospital in Rotterdam for Investigation and Treatment of TCFA (SECRITT). EuroIntervention. 2012;8:945–54.
49.• Brugaletta S, Radu MD, Garcia-Garcia HM, et al. Circumferential evaluation of the neointima by optical coherence tomography after ABSORB bioresorbable vascular scaffold implantation: can the scaffold cap the plaque? Atherosclerosis. 2012;221:106–12. *Interesting original paper exploring the possibility of using neointimal growth to modify plaque stability.*
50. Brezinski ME. Current capabilities and challenges for optical coherence tomography as a high-impact cardiovascular imaging modality. Circulation. 2011;123:2913–5.
51. Radu MD, Falk E. In search of vulnerable features of coronary plaques with optical coherence tomography: is it time to rethink the current methodological concepts? Eur Heart J. 2012;33:9–12.
52. Kawasaki M, Bouma BE, Bressner J, et al. Diagnostic accuracy of optical coherence tomography and integrated backscatter intravascular ultrasound images for tissue characterization of human coronary plaques. J Am Coll Cardiol. 2006;48:81–8.
53. Manfrini O, Mont E, Leone O, et al. Sources of error and interpretation of plaque morphology by optical coherence tomography. Am J Cardiol. 2006;98:156–9.
54. Goderie TP, van Soest G, Garcia-Garcia HM, et al. Combined optical coherence tomography and intravascular ultrasound radio frequency data analysis for plaque characterization. Classification accuracy of human coronary plaques in vitro. Int J Cardiovasc Imaging. 2010;26:843–50.
55. Xu C, Schmitt JM, Carlier SG, Virmani R. Characterization of atherosclerosis plaques by measuring both backscattering and attenuation coefficients in optical coherence tomography. J Biomed Opt. 2008;13:034003.
56.• van Soest G, Regar E, Goderie TP, et al. Pitfalls in plaque characterization by OCT: image artifacts in native coronary arteries. JACC Cardiovasc Imaging. 2011;4:810–3. *This paper highlights the importance of understanding how various artefacts may affect plaque characterization.*
57.• Radu MD, Räber L, Serruys PW. Artefacts with Intracoronary Optical Coherence Tomography. In: Radu MD, Räber L, Garcia-Garcia HM, et al, editors. The Clinical Atlas of Intravascular Optical Coherence Tomography. Toulouse: Europa Edition; 2012. *This document contains a wide source of OCT images with focus on image interpretation.*
58.•• Tearney GJ, Regar E, Akasaka T, et al. Consensus standards for acquisition, measurement, and reporting of intravascular optical coherence tomography studies: a report from the international working group for intravascular optical coherence tomography standardization and validation. J Am Coll Cardiol. 2012;59: 1058–72. *This consensus document can be used as standard reference regarding the current state of OCT.*
59. Räber L, Heo JH, Radu MD, et al. Offline fusion of co-registered intravascular ultrasound and frequency domain optical coherence tomography images for the analysis of human atherosclerotic plaques. EuroIntervention. 2012;8:98–108.
60. van Soest G, Goderie T, Regar E, et al. Atherosclerotic tissue characterization in vivo by optical coherence tomography attenuation imaging. J Biomed Opt. 2010;15:011105.
61. Wang Z, Chamie D, Bezerra HG, et al. Volumetric quantification of fibrous caps using intravascular optical coherence tomography. Biomed Opt Express. 2012;3:1413–26.
62. Stone GW, Moses JW, Ellis SG, et al. Safety and efficacy of sirolimus- and paclitaxel-eluting coronary stents. N Engl J Med. 2007;356:998–1008.

63. Virmani R, Kolodgie FD, Farb A, et al. Drug eluting stents: are human and animal studies comparable? Heart. 2003;89:133–8.
64. van Werkum JW, Heestermans AA, de Korte FI, et al. Long-term clinical outcome after a first angiographically confirmed coronary stent thrombosis: an analysis of 431 cases. Circulation. 2009;119: 828–34.
65. Räber L, Magro M, Stefanini GG, et al. Very late coronary stent thrombosis of a newer-generation everolimus-eluting stent compared with early-generation drug-eluting stents: a prospective cohort study. Circulation. 2012;125:1110–21.
66. Cutlip DE, Windecker S, Mehran R, et al. Clinical end points in coronary stent trials: a case for standardized definitions. Circulation. 2007;115:2344–51.
67. Alfonso F, Suarez A, Angiolillo DJ, et al. Findings of intravascular ultrasound during acute stent thrombosis. Heart. 2004;90:1455–9.
68. Finn AV, Joner M, Nakazawa G, et al. Pathological correlates of late drug-eluting stent thrombosis: strut coverage as a marker of endothelialization. Circulation. 2007;115:2435–41.
69. Cook S, Wenaweser P, Togni M, et al. Incomplete stent apposition and very late stent thrombosis after drug-eluting stent implantation. Circulation. 2007;115:2426–34.
70. Kang SJ, Lee CW, Song H, et al. OCT analysis in patients with very late stent thrombosis. JACC Cardiovasc Imaging. 2013;6: 695–703.
71. Amabile N, Souteyrand G, Ghostine S, et al. Very late stent thrombosis related to incomplete neointimal coverage or neoatherosclerotic plaque rupture identified by optical coherence tomography imaging. Eur Heart J Cardiovasc Imaging. 2014;15: 24–31.
72. Park SJ, Kim YH, Park DW, et al. Impact of intravascular ultrasound guidance on long-term mortality in stenting for unprotected left main coronary artery stenosis. Circ Cardiovasc Interv. 2009;2: 167–77.
73. Räber L, Windecker S. IVUS-guided percutaneous coronary interventions: an ongoing odyssey? Circulation. 2014;129:417–9.
74.• Guagliumi G, Sirbu V, Musumeci G, et al. Examination of the in vivo mechanisms of late drug-eluting stent thrombosis: findings from optical coherence tomography and intravascular ultrasound imaging. JACC Cardiovasc Interv. 2012;5:12–20. *This study is the first systematic evaluation of late stent thrombosis using OCT.*
75. Nakazawa G, Otsuka F, Nakano M, et al. The pathology of neoatherosclerosis in human coronary implants bare-metal and drug-eluting stents. J Am Coll Cardiol. 2011;57:1314–22.
76. Imola F, Mallus MT, Ramazzotti V, et al. Safety and feasibility of frequency domain optical coherence tomography to guide decision making in percutaneous coronary intervention. EuroIntervention. 2010;6:575–81.
77. Viceconte N, Chan PH, Barrero EA, et al. Frequency domain optical coherence tomography for guidance of coronary stenting. Int J Cardiol. 2013;166:722–8.
78. Prati F, Di Vito L, Biondi-Zoccai G, et al. Angiography alone versus angiography plus optical coherence tomography to guide decision-making during percutaneous coronary intervention: the Centro per la Lotta contro l'Infarto-Optimisation of Percutaneous Coronary Intervention (CLI-OPCI) study. EuroIntervention. 2012;8:823–9.
79. Di Giorgio A, Capodanno D, Ramazzotti V, et al. Optical coherence tomography guided in-stent thrombus removal in patients with acute coronary syndromes. Int J Cardiovasc Imaging. 2013;29:989–96.
80. Cutlip DE, Baim DS, Ho KK, et al. Stent thrombosis in the modern era: a pooled analysis of multicenter coronary stent clinical trials. Circulation. 2001;103:1967–71.
81. Biondi-Zoccai GG, Agostoni P, Sangiorgi GM, et al. Incidence, predictors, and outcomes of coronary dissections left untreated after drug-eluting stent implantation. Eur Heart J. 2006;27:540–6.
82. Cheneau E, Leborgne L, Mintz GS, et al. Predictors of subacute stent thrombosis: results of a systematic intravascular ultrasound study. Circulation. 2003;108:43–7.
83. Gonzalo N, Serruys PW, Okamura T, et al. Optical coherence tomography assessment of the acute effects of stent implantation on the vessel wall: a systematic quantitative approach. Heart. 2009;95:1913–9.
84. Gonzalo N, Serruys PW, Okamura T, et al. Relation between plaque type and dissections at the edges after stent implantation: an optical coherence tomography study. Int J Cardiol. 2011;150: 151–5.
85. Kume T, Okura H, Miyamoto Y, et al. Natural history of stent edge dissection, tissue protrusion and incomplete stent apposition detectable only on optical coherence tomography after stent implantation. Circ J. 2012;76:698–703.
86. Radu MD, Raber L, Heo J, et al. Natural history of optical coherence tomography-detected non-flow-limiting edge dissections following drug-eluting stent implantation. EuroIntervention. 2014;9: 1085–9.
87. Reith S, Battermann S, Jaskolka A, et al. Predictors and incidence of stent edge dissections in patients with type 2 diabetes as determined by optical coherence tomography. Int J Cardiovasc Imaging. 2013;29:1237–47.
88. Kawamori H, Shite J, Shinke T, et al. Natural consequence of post-intervention stent malapposition, thrombus, tissue prolapse, and dissection assessed by optical coherence tomography at mid-term follow-up. Eur Heart J Cardiovasc Imaging. 2013;14:865–75.
89. Chamie D, Bezerra HG, Attizzani GF, et al. Incidence, predictors, morphological characteristics, and clinical outcomes of stent edge dissections detected by optical coherence tomography. JACC Cardiovasc Interv. 2013;6:800–13.
90. Christensen R, Holm NR, Orhoj T, et al. TCT-297 Stent edge dissections detected by optical coherence tomography: incidence, predictors and 12-month outcome. J Am Coll Cardiol. 2012;60: 17S.
91. Sheris SJ, Canos MR, Weissman NJ. Natural history of intravascular ultrasound-detected edge dissections from coronary stent deployment. Am Heart J. 2000;139(1 Pt 1):59–63.
92. Liu X, Tsujita K, Maehara A, et al. Intravascular ultrasound assessment of the incidence and predictors of edge dissections after drug-eluting stent implantation. JACC Cardiovasc Interv. 2009;2:997–1004.
93. De Cock D, Bennet J, Ughi GJ, et al. EuroPCR-357 Healing course of tissue prolapse and intra-stent dissection after PCI: a sequential OCT study. EuroIntervention. 2013;EuroPCR 2013 [Abstracts].
94. Hassan AK, Bergheanu SC, Stijnen T, et al. Late stent malapposition risk is higher after drug-eluting stent compared with bare-metal stent implantation and associates with late stent thrombosis. Eur Heart J. 2009;31:1172–80.
95. Gonzalo N, Barlis P, Serruys PW, et al. Incomplete stent apposition and delayed tissue coverage are more frequent in drug-eluting stents implanted during primary percutaneous coronary intervention for ST-segment elevation myocardial infarction than in drug-eluting stents implanted for stable/unstable angina: insights from optical coherence tomography. JACC Cardiovasc Interv. 2009;2:445–52.
96.• Ozaki Y, Okumura M, Ismail TF, et al. The fate of incomplete stent apposition with drug-eluting stents: an optical coherence tomography-based natural history study. Eur Heart J. 2010;31: 1470–6. *This study provides important information about the healing of malapposed struts.*
97. Kubo T, Imanishi T, Kitabata H, et al. Comparison of vascular response after sirolimus-eluting stent implantation between patients with unstable and stable angina pectoris: a serial optical coherence tomography study. JACC Cardiovasc Imaging. 2008;1:475–84.

98. Tanigawa J, Barlis P, Dimopoulos K, et al. The influence of strut thickness and cell design on immediate apposition of drug-eluting stents assessed by optical coherence tomography. Int J Cardiol. 2009;134:180–8.
99. Tanigawa J, Barlis P, Dimopoulos K, et al. Optical coherence tomography to assess malapposition in overlapping drug-eluting stents. EuroIntervention. 2008;3:580–3.
100. Lindsay AC, Paulo M, Kadriye K, et al. Predictors of stent strut malapposition in calcified vessels using frequency-domain optical coherence tomography. J Invasive Cardiol. 2013;25:429–34.
101. Gomez-Lara J, Radu M, Brugaletta S, et al. Serial analysis of the malapposed and uncovered struts of the new generation of everolimus-eluting bioresorbable scaffold with optical coherence tomography. JACC Cardiovasc Interv. 2011;4:992–1001.
102.• Gutierrez-Chico JL, Regar E, Nuesch E, et al. Delayed coverage in malapposed and side-branch struts with respect to well-apposed struts in drug-eluting stents: in vivo assessment with optical coherence tomography. Circulation. 2011;124:612–23. *This study provides important information on the impact of apposition on healing*.
103. Gutierrez-Chico JL, Wykrzykowska J, Nuesch E, et al. Vascular tissue reaction to acute malapposition in human coronary arteries: sequential assessment with optical coherence tomography. Circ Cardiovasc Interv. 2012;5(20–9):S21–8.
104. Mintz GS. What to do about late incomplete stent apposition? Circulation. 2007;115:2379–81.
105. Guagliumi G, Sirbu V, Musumeci G, et al. Strut coverage and vessel wall response to a new-generation paclitaxel-eluting stent with an ultrathin biodegradable abluminal polymer: Optical Coherence Tomography Drug-Eluting Stent Investigation (OCTDESI). Circ Cardiovasc Interv. 2010;3:367–75.
106. Barlis P, Regar E, Serruys PW, et al. An optical coherence tomography study of a biodegradable vs durable polymer-coated limus-eluting stent: a LEADERS trial sub-study. Eur Heart J. 2010;31:165–76.
107. Guagliumi G, Costa MA, Sirbu V, et al. Strut coverage and late malapposition with paclitaxel-eluting stents compared with bare metal stents in acute myocardial infarction: optical coherence tomography substudy of the Harmonizing Outcomes with Revascularization and Stents in Acute Myocardial Infarction (HORIZONS-AMI) Trial. Circulation. 2011;123:274–81.
108. Gutierrez-Chico JL, van Geuns RJ, Regar E, et al. Tissue coverage of a hydrophilic polymer-coated zotarolimus-eluting stent vs a fluoropolymer-coated everolimus-eluting stent at 13-month follow-up: an optical coherence tomography substudy from the RESOLUTE All Comers trial. Eur Heart J. 2011;32:2454–63.
109. Räber L, Baumgartner S, Garcia HM, et al. Long-term vascular healing in response to sirolimus- and paclitaxel-eluting stents: an optical coherence tomography study. JACC Cardiovasc Interv. 2012;5:946–57.
110. Prati F, Zimarino M, Stabile E, et al. Does optical coherence tomography identify arterial healing after stenting? An in vivo comparison with histology, in a rabbit carotid model. Heart. 2008;94:217–21.
111. Finn AV, Nakazawa G, Joner M, et al. Vascular responses to drug eluting stents: importance of delayed healing. Arterioscler Thromb Vasc Biol. 2007;27:1500–10.
112. Murata A, Wallace-Bradley D, Tellez A, et al. Accuracy of optical coherence tomography in the evaluation of neointimal coverage after stent implantation. JACC Cardiovasc Imaging. 2010;3:76–84.
113.• Templin C, Meyer M, Muller MF, et al. Coronary optical frequency domain imaging (OFDI) for in vivo evaluation of stent healing: comparison with light and electron microscopy. Eur Heart J. 2010;31:1792–801. *This study provides insights into the importance of using the OCT signal for correct tissue characterization, and may be used for future automatic segmentation algorithms*.
114. Gutierrez-Chico JL, Alegria-Barrero E, Teijeiro-Mestre R, et al. Optical coherence tomography: from research to practice. Eur Heart J Cardiovasc Imaging. 2012;13:370–84.
115. Otsuka F, Nakano M, Vorpahl M, et al. Pathology of second- versus first-generation drug-eluting stents in humans: does safety issue still exist? Eur Heart J. 2011;32(Abstract Suppl):82.
116. Nakano M, Vorpahl M, Otsuka F, et al. Ex vivo assessment of vascular response to coronary stents by optical frequency domain imaging. JACC Cardiovasc Imaging. 2012;5:71–82.
117. Radu M, Jorgensen E, Kelbaek H, et al. Optical coherence tomography at follow-up after percutaneous coronary intervention: relationship between procedural dissections, stent strut malapposition and stent healing. EuroIntervention. 2011;7:353–61.
118. Joner M, Finn AV, Farb A, et al. Pathology of drug-eluting stents in humans: delayed healing and late thrombotic risk. J Am Coll Cardiol. 2006;48:193–202.
119. Radu MD, Raber L, Kalesan B, et al. Coronary evaginations are associated with positive vessel remodeling and are nearly absent following implantation of newer-generation drug-eluting stents: an optical coherence tomography and intravascular ultrasound study. Eur Heart J. 2014;35:795–807.
120. Radu MD, Pfenniger A, Raber L, et al. Flow disturbances in stent-related coronary evaginations: a computational fluid-dynamic simulation study. EuroIntervention. 2014;10:113–23.
121. Imai M, Kadota K, Goto T, et al. Incidence, risk factors, and clinical sequelae of angiographic peri-stent contrast staining after sirolimus-eluting stent implantation. Circulation. 2011;123:2382–91.
122. Ughi GJ, Adriaenssens T, Onsea K, et al. Automatic segmentation of in-vivo intra-coronary optical coherence tomography images to assess stent strut apposition and coverage. Int J Cardiovasc Imaging. 2012;28:229–41.